Marine Biology (2006) 149: 1325–1335
DOI 10.1007/s00227-006-0286-4

RESEARCH ARTICLE

K. E. Ulstrup · P. J. Ralph · A. W. D. Larkum
M. Kühl

Intra-colonial variability in light acclimation of zooxanthellae in coral tissues of *Pocillopora damicornis*

Received: 6 September 2005 / Accepted: 6 February 2006 / Published online: 3 May 2006

Abstract We investigated heterogeneity of light acclimation of photosynthesis in sun- and shade-adapted coenosarc and polyp tissues of *Pocillopora damicornis*. The zooxanthellar community within *P. damicornis* colonies at Heron Island is genetically uniform, yet they showed a large degree of plasticity in their photo-physiological acclimation linked to light microclimates characterised by fibre-optic microprobes. Microscale scalar irradiance measurements showed higher absorption in polyp than coenosarc tissues and higher absorption in the more densely pigmented shade-adapted polyps than in sun-adapted polyps. The combination of an O_2 microelectrode with a fibre-optic microprobe (combined sensor diameter 50–100 μm) enabled parallel measurements of O_2 concentration, gross photosynthesis rate and photosystem II (PSII) quantum yield at the coral surface under steady-state conditions as a function of increasing irradiances. Lower O_2 levels at the tissue surface and higher compensation irradiance indicated a higher respiration activity in sun-adapted polyp tissue as compared to shade-adapted polyps. Shade-adapted coenosarc and polyp tissues exhibited lower maxima of relative electron transport rates ($rETR_{max}$) (84 ± 15 and 41 ± 10, respectively) than sun-adapted coenosarc and polyp tissues (136 ± 14 and 77 ± 13, respectively). Shade-adapted tissues showed stronger decrease of rETR at high scalar irradiances as compared to sun-adapted tissues. The relationship between the relative PSII electron transport and the rate of gross photosynthesis, as well as O_2 concentration, was non-linear in sun-adapted tissues over the entire irradiance range, whereas for shade-adapted tissues the relationship became non-linear at medium to high scalar irradiances > 200 μmol photons m^{-2} s^{-1}. This suggests that rETR measurements should be used with caution in corals as a proxy for photosynthesis rates. The apparently high rates of photosynthesis (oxygen evolution rates) suggest that there must be a considerable electron transport rate through the photosystems that is not observed by the rETR measurements. This may be accounted for by vertical heterogeneity of zooxanthellae in the tissue and the operation of an alternative electron pathway such as cyclic electron flow around PSII.

Communicated by G.F. Humphrey, Sydney

K. E. Ulstrup · P. J. Ralph (✉)
Department of Environmental Science,
Institute for Water and Environmental Resource Management,
University of Technology, PO Box 123 Broadway, 2007 Sydney,
NSW, Australia
E-mail: peter.ralph@uts.edu.au
Tel.: +61-2-95144070
Fax: +61-2-95144003

A. W. D. Larkum
School of Biological Sciences, University of Sydney,
2006 Sydney, NSW, Australia

M. Kühl
Marine Biological Laboratory, Institute of Biology,
University of Copenhagen, Strandpromenaden 5,
3000 Helsingor, Denmark

Introduction

Reef-building corals are sessile marine cnidarians that harbour endosymbiotic microalgae of the dinoflagellate genus *Symbiodinium*, known as zooxanthellae. The dynamic relationship between production and consumption of O_2 in corals is regulated through the photosynthetic activity of the zooxanthellae, the respiration of the zooxanthellae and their hosts and solute exchange across diffusive boundary layers (DBLs) (Shashar et al. 1993; Kühl et al. 1995). Corals are subject to limited gas exchange with the surrounding seawater across a DBL, causing severe hypoxia in the dark due to the absence of light-driven photosynthesis, while O_2 supersaturation is common during exposure to high light (Kühl et al. 1995; Ulstrup et al. 2005). The light intensity and spectrum reaching the zooxanthellae, and the solute exchange

between the coral and the surrounding seawater are the most important external regulators of photosynthesis (Dubinsky et al. 1984; Patterson et al. 1991; Kühl et al. 1995).

The photosynthetic capacity of zooxanthellae as measured by variable fluorescence is commonly used as a proxy for the health of the coral (Warner et al. 1999; Bhagooli and Hidaka 2003). Decreased zooxanthellar productivity has been correlated to episodes of coral bleaching, a process in which corals lose their symbionts and/or pigments and subsequently may perish (Hoegh-Guldberg 1999; Marshall and Baird 2000). It has also been speculated that genetically distinct zooxanthellae may exhibit differences in their photosynthetic capacity and tolerance towards bleaching conditions (Buddemeier and Fautin 1993; Baker et al. 2004).

Variable chlorophyll *a* fluorescence analysis has shown differences in photosynthetic performance between upper and lower surfaces of individual colonies (Jones et al. 1998; Ralph et al. 2005), between polyp and coenosarc tissue (Ralph et al. 2002; Hill et al. 2004), and along the length of coral branches (Hill et al. 2004). Kühl et al. (1995) showed significant variation of gross photosynthetic activity between polyp and coenosarc tissue of *Favia* sp. due to differences in boundary layers and light microclimate within a single polyp. The scalar irradiance, i.e. the spherically integrated quantum flux from all directions about a point, can locally exceed the incident downwelling irradiance (E_d) in corals due to intense scattering and light trapping in the tissue and skeleton (Kühl et al. 1995; Enriquez et al. 2005). The large heterogeneity of the physico-chemical microenvironment within corals can lead to different responses of photo-acclimation and -adaptation in different parts of the coral colony (Falkowski et al. 1990; Jones et al. 1998; Ralph et al. 2002).

Oxygen microelectrodes enable fine-scale studies of gross photosynthetic activity using the light–dark shift technique (Revsbech and Jørgensen 1983) at the surface of coral tissue, where the photosynthesis of the zooxanthellae can be assessed with this technique independent of host or symbiont respiration (Kühl et al. 1995; De Beer et al. 2000). Variable chlorophyll *a* fluorescence analysis with fibre-optic microprobes (Schreiber et al. 1996; Kühl et al. 2005) can also be used to map photosynthesis and light acclimation at high spatial resolution in corals (Ralph et al. 2002).

Oxygen microsensor techniques enable measurements of gross photosynthesis rate vs. irradiance curves over different time scales. The measurement of gross photosynthesis rate with oxygen microsensors has a spatial resolution of ~0.1 mm and assumes steady-state O_2 distribution before the light–dark shift (Revsbech and Jørgensen 1983; Kühl et al. 1996). Steady-state conditions at the point of measurement thus reflect a balance between O_2 transport, consumption and production, which is obtained when acclimation to a particular light intensity has occurred and no further changes to the O_2 level are detected. Similarly, the effective quantum yield of photosystem II (PSII) and the relative photosynthetic electron transport rate at steady-state, under a range of irradiances, can be measured with pulse-amplitude-modulated (PAM) fluorometers using the saturation-pulse technique (Schreiber 2004). Measurements of steady-state photosynthesis vs. irradiance curves typically involve incubation for 10–60 min at each irradiance level. This time interval is long enough to allow for photo-acclimation during incubation (Kühl et al. 2001) and may also lead to greater photo-inactivation above saturating irradiance due to the prolonged light exposure.

Another way of investigating the photosynthetic capacity of corals is to measure so-called rapid light curves (RLC), where quantum yields and relative photosynthetic electron transport are measured rapidly over a range of irradiances using only very brief (10–20 s) incubation periods for each irradiance (Schreiber 2004). RLC, obtained over a few minutes, provide insight into the momentary acclimation capacity for light utilisation of PSII (Ralph and Gademann 2005) and should not be interpreted as steady-state photosynthesis vs. irradiance curves.

In this study, we investigated the branching coral *Pocillopora damicornis*. The population of *P. damicornis* in the Heron Island lagoon has been found to harbour only one strain of zooxanthellae belonging to clade C (LaJeunesse et al. 2003; Ulstrup et al. 2006), as confirmed by denaturing gradient gel electrophoresis and single-stranded conformation polymorphism, respectively, followed by DNA sequencing. This coral population is therefore suitable to assess intra-colonial variation of zooxanthellar physiology without complications of underlying genetic variation. The branching morphology induces a heterogenous light climate across the colony where basal parts of the colony are shaded by exposed branches at a scale of millimetres to centimetres (Ralph et al. 2005). However, the ambient light climate is also variable at a much finer scale (μm–mm) as a result of structural heterogeneities of the skeleton and tissue, such as those observed between polyp and coenosarc tissue (Kühl et al. 1995; Enriquez et al. 2005). Physiological responses may thus correlate to tissue type as well as to light microclimate (Ralph et al. 2002).

Here we present the first direct microscale comparison of oxygen- and variable fluorescence-based measures of coral photosynthesis, as determined with a novel combined microsensor consisting of an O_2 microelectrode and a fibre-optic microprobe (Kühl 2005). We examined the gross photosynthesis and steady-state PSII quantum yields of zooxanthellae harboured in sun- and shade-adapted regions of coenosarc and polyp tissue in individual colonies of the scleractinian coral *P. damicornis* at Heron Island on the southern Great Barrier Reef. Our results show that variable fluorescence data obtained in corals cannot be directly correlated to productivity, especially at higher irradiances.

Materials and methods

Sampling and experimental setup

Samples were collected in the Heron Island lagoon (< 2 m depth) adjacent to Heron Island Research Station (152°06′E, 20°29′S) during January 2005. Sun- and shade-adapted fragments of *P. damicornis* colonies were collected and maintained in flow-through aquaria under shaded conditions (< 50 µmol photons m^{-2} s^{-1} for 1 day. Samples were held securely in plasticine within a custom-built flow chamber 25 cm × 10 cm × 10 cm at a flow velocity of ~1 cm s^{-1}. A combined O_2 microelectrode and tapered fibre-optic microsensor with a combined sensor diameter of 50–100 µm (Kühl 2005) was used to conduct simultaneous measurements of O_2 concentration, gross photosynthesis rate and PSII fluorescence yield (maximum quantum yield in the dark, effective quantum yield in the light) at the surface of the coral.

The O_2 microelectrode was connected to a picoamperemeter (PA2000, Unisense, Århus, Denmark). Measuring signals were recorded on a strip chart recorder (Kipp & Zonen, Holland) and linear calibration of the electrode was performed at an ambient temperature of 26.5 ± 0.5°C by recording signals in air-saturated seawater and O_2-free seawater, respectively. The O_2 concentration of air-saturated seawater at experimental temperature and salinity, i.e. 208 µmol O_2 l^{-1} was obtained from tabulated values (http://www.unisense.com/support/support.html). The fibre-optic microprobe was connected to a PAM fluorometer (Microfibre-PAM, Walz, Germany). The fluorometer also controlled a red light emitting diode (LED 650 nm)-ring, which was used as an actinic light source. The fluorometer was interfaced to a windows-based PC and the system software (WinControl software v2.08, Walz, Germany) allowed monitoring of fluorescence in real time and acquisition of fluorescence parameters at defined irradiance and time intervals. The combined microsensor was positioned through the centre of the LED-ring, which illuminated the coral sample with actinic light from oblique angles, thus minimising any self-shadowing effects on the measurements (Fig. 1). The microsensor was placed in direct contact with the coenosarc tissue surface or inside a polyp between 5 and 10 mm from the coral branch tip using a manual micromanipulator (MM33, Märtzhäuser, Germany). The microsensor was positioned while observing the sample with a dissecting microscope (Leica, Germany).

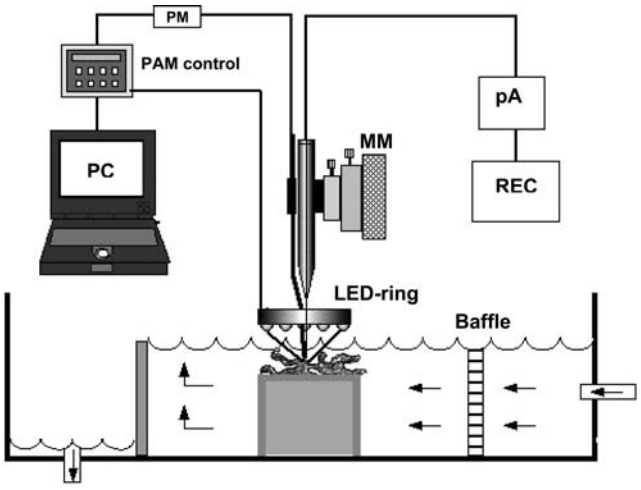

Fig. 1 Scheme of experimental setup for combined microsensor measurements of oxygen and variable chlorophyll *a* fluorescence. The combined microsensor is mounted on a micromanipulator (*MM*). The O_2 microelectrode part of the sensor is connected to a picoamperemeter (*pA*) and the sensor signal is recorded on a strip chart recorder (*REC*). The fibre-optic microprobe part of the sensor is connected to a photomultiplier detector unit (*PM*), which is connected to a PC-interfaced controlling unit (*PAM control*). The photomultiplier detector unit and the LED-ring, which served as an actinic light source, were also connected to the controlling unit

Scalar irradiance

Scalar irradiance spectra (450–750 nm) were measured with a fibre-optic microprobe ~0.1 mm in diameter (Lassen et al. 1992) connected to a high spectral resolution diode-array detector (PMA-11, Hamamatsu Photonics, Hamamatsu, Japan). The tip of the microprobe was placed on the surface of the coenosarc tissue or inserted into a polyp using a micromanipulator and a dissecting microscope. The probe was advanced to the tissue at a zenith angle of ~135–145° relative to the vertically incident light. A fibre-optic light source (Schott KL-2500, Mainz, Germany) with a 250-W halogen lamp (Xenophot, Osram, Germany) and fitted with a collimating lens was used for homogeneous, vertical illumination of the coral samples. Once the polyp tentacles engulfed the probe (usually after a few minutes), the measurement was performed. Scalar irradiance measurements were related to the incident downwelling irradiance measured over a black non-reflective surface to reduce stray light and reflection of light. Three haphazardly chosen areas of coenosarc and polyp tissues in sun- and shade-adapted regions, respectively, were measured. All measurements were performed in a darkened room at < 1 µmol photons m^{-2} s^{-1}. The scalar irradiance measurements were used to correct the known levels of actinic incident irradiance used in the microsensor measurements of gross photosynthesis rate and variable fluorescence to tissue scalar irradiance.

Measuring sequence

A batch program (WinControl) was written to automate the incremental change in actinic light from the LED-ring, which had been calibrated against a quantum irradiance metre (Li-Cor, Lincoln, NE, USA) with a

quantum sensor (Li-190SA). Each of eight actinic irradiances (0, 25, 50, 100, 170, 240, 470, 1,100 µmol photons m^{-2} s^{-1}) were applied for 10 min in order to obtain steady-state conditions prior to O_2 and variable chlorophyll *a* fluorescence measurements (Fig. 2). Ten minutes was found to be sufficient time to reach steady-state levels of O_2 and fluorescence yields, as monitored using the strip chart recorder and the WinControl chart function, respectively (data not shown). The O_2 concentration was then recorded and a saturating light pulse was applied to obtain the fluorescence-based quantum yields of PSII. Thereafter, a light–dark shift was applied to measure the gross photosynthesis rate (Fig. 2). The light–dark shift technique is based on the assumption that the immediate O_2 depletion following the light–dark shift is equal to the photosynthetic O_2 production during the previous light period (Revsbech and Jørgensen 1983). Due to the high spatial resolution along with the low stirring sensitivity and fast response time of the O_2 microelectrodes (Revsbech 1989), we were able to measure the gross photosynthesis rate (nmol O_2 cm^{-3} s^{-1}) at ~100 µm spatial resolution by measuring the rate of O_2 depletion immediately after darkening.

Fluorescence yields were measured on both dark-acclimated (maximum F_m, minimum F_o) and light-acclimated (effective maximum F_m', minimum F_t) samples (see Schreiber 2004 for review). The steady-state measurements were performed after a 10-min initial dark period to obtain the maximum quantum yield of PSII, $F_v/F_m = (F_m - F_o)/F_m$, and after each of the following seven actinic irradiance steps which provided an estimate of the effective quantum yield of PSII, $\Phi_{PSII} = (F_m' - F_t)/F_m'$. Non-photochemical quenching, NPQ = $(F_m - F_m')/F_m'$, was determined at an intermediate scalar irradiance. NPQ for sun- and shade-adapted coenosarc tissues was determined at 358 and 328 µmol photons m^{-2} s^{-1}, respectively, whereas NPQ for sun- and shade-adapted polyp tissues was determined at 406 and 290 µmol photons m^{-2} s^{-1}, respectively. The rETR was calculated as rETR = $E_0 \times \Phi_{PSII}$ (Ralph et al. 2002), where E_0 is the scalar irradiance. Information about the partitioning of light energy between PSI and PSII, as well as the absorption cross-section of PSII would be necessary in order to determine absolute ETR values (Schreiber 2004; Ralph and Gademann 2005). The settings of the Microfibre-PAM were adjusted so that a fluorescence signal above 100 units on dark-acclimated samples was obtained (photomultiplier gain 30, output gain 8 and measuring light 8).

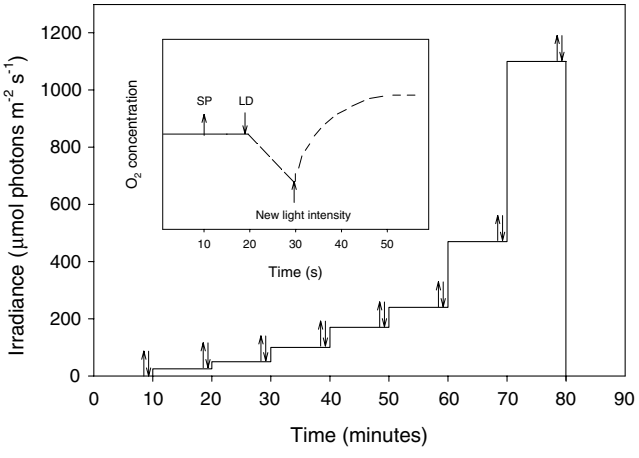

Fig. 2 Schematic illustration of the measuring sequence for obtaining a combined steady-state *P* vs. actinic irradiance and relative electron transport rate vs. irradiance curve. Steady-state in levels of oxygen and fluorescence yields were obtained after 10 min at each irradiance level (*stepped curve*). At the end of each 10-min period a saturating pulse was applied (*SP*, *up arrow*) followed by a light–dark shift (*LD*, *down arrow*). *Inset* shows the saturating pulse (SP), light–dark shift (LD) and the subsequent increase of irradiance. The sequence was completed within 30 s at the end of each 10 min steady-state acclimation period

Curve fitting

The functions of Platt et al. (1980) were fitted to rETR vs. scalar irradiance and gross photosynthesis vs. scalar irradiance data derived from steady-state measurements in order to quantitatively compare their descriptive parameters [fluorescence—maximum rETR ($rETR_{max}$), initial slope (α_f) and minimum saturating scalar irradiance (E_{kf}); gross photosynthesis rate—maximum gross photosynthesis rate (Pg_{max}), initial slope (α_{Pg}) and minimum saturating scalar irradiance (E_{kPg})]. Fitted curves were derived from the empirical data (Sigmaplot v6.1, Systat, Richmond, CA, USA). For further details see Kühl et al. (2001) and Ralph et al. (2002).

Statistical analysis

Sun- and shade-adapted surfaces of coenosarc and polyp tissues were tested for statistical independency using Pearson's correlation. Assumptions of normality and equal variances were satisfied, thus validating the use of a one-way analysis of variance for all comparisons of $rETR_{max}$, α_f, E_{kf}, Pg_{max}, α_{Pg} and E_{kPg} as well as for F_v/F_m, Φ_{PSII} and NPQ. The non-parametric Kruskal–Wallis test was performed where normality and equal variance were not achieved. Statistical analyses were performed using SPSS software v11.0.0 (USA).

Results

Spectral scalar irradiance measurements at the tissue surface showed only minor differences between coenosarc tissues in sun- and shade-adapted regions of corals. However, when the microprobe was inserted into the polyp tissue, shade-adapted polyps showed much lower light penetration than in the sun-adapted polyps (Fig. 3). Polyps exhibited a strong absorption of chlorophyll *a* as seen by a pronounced spectral trough at 675 nm in both sun- and shade-adapted polyps.

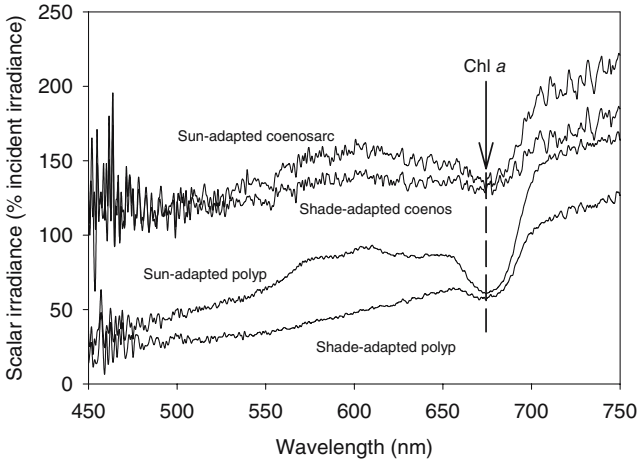

Fig. 3 Spectral scalar irradiance measurements of sun- and shade-adapted polyp tissues of *Pocillopora damicornis*. Data are normalised to the incident downwelling scalar irradiance (E_d). *Arrow* indicates the absorption wavelength of chlorophyll *a* (675 nm)

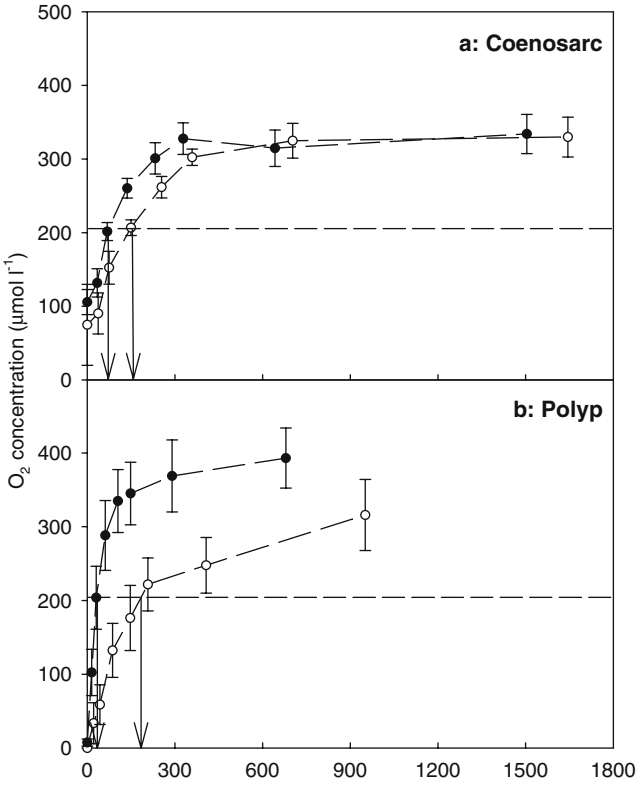

Fig. 4 Steady-state levels of O_2 concentration at the surface of sun- (*empty circle*) and shade-adapted (*filled circle*) coenosarc (**a**) and polyp (**b**) tissues of *Pocillopora damicornis* ($n = 5 \pm$ SE) in response to increasing scalar irradiance. *Arrows* indicate the compensation irradiance (E_c), above which the oxygen level at the tissue surface exceeds the level of the overlaying air-saturated seawater (208 µmol l^{-1})

Sun- and shade-adapted coenosarc tissue showed a minimum of approximately 120% and a maximum of approximately 180% of incident downwelling irradiance in the visible spectral region (500–700 nm). The scalar irradiance at 650 nm of sun- and shade-adapted polyp tissue was 86 and 62%, respectively. In sun- and shade-adapted coenosarc tissue the scalar irradiance amounted to 137 and 150%, respectively, of incident downwelling irradiance (Fig. 3).

Sun- and shade-adapted coenosarc tissues as well as shade-adapted polyp tissues exhibited similar maximal O_2 concentration levels (Fig. 4a, b). At the highest scalar irradiance (951 µmol photons m^{-2} s^{-1}) sun-adapted polyps exhibited a lower O_2 concentration (316 ± 48 µmol L^{-1}), whereas shade-adapted polyps exposed maximally to 679 µmol photons m^{-2} s^{-1} exhibited an O_2 concentration level of 393 ± 41 µmol L^{-1} (Fig. 4b). In the dark, the O_2 concentration in coenosarc tissue decreased to $< 50\%$ of that in the air-saturated surrounding seawater (75 ± 56 µmol L^{-1} in sun-adapted regions and 106 ± 17 µmol l^{-1} in shade-adapted regions) due to respiration coupled with mass transfer limitation imposed by the DBL (Fig. 4a). Polyp tissues were almost completely hypoxic in darkness as the O_2 concentration decreased to < 2 µmol L^{-1} at the tissue surface (Fig. 4b). The compensation irradiance, E_c, i.e. the irradiance above which the tissue exhibits net oxygen production, was higher in sun-adapted polyps (E_c ~190 µmol photons m^{-2} s^{-1}) than in sun-adapted coenosarc tissues (E_c ~160 µmol photons m^{-2} s^{-1}). Shade-adapted polyp and coenosarc tissues exhibited a compensation irradiance of ~40 and 70 µmol photons m^{-2} s^{-1}, respectively (Fig. 4a, b).

Effective quantum yields were significantly higher ($P < 0.001$) in sun-adapted than in shade-adapted coenosarc tissues. There were no significant difference in maximum quantum yield ($P = 0.064$) and non-photochemical quenching ($P = 0.092$) between tissue types (Table 1).

The fluorescence-based steady-state rETR vs. scalar irradiance curve showed higher maximal rETR in sun-adapted regions than in shade-adapted regions of polyp tissues ($P < 0.001$) (Table 2; Fig. 5c, d). Also, α_f was significantly higher in shade-adapted tissues than in sun-adapted tissues ($P = 0.023$) as was E_{kf} ($P = 0.016$). These observations are typical of high- and low-light adapted photosystems. In sun-adapted coenosarc and polyp tissues as well as shade-adapted polyp tissue gross photosynthesis rates continued to rise at high scalar irradiances whereas rETR became inhibited in all cases at scalar irradiances > 300 µmol photons m^{-2} s^{-1} (Fig. 5a–d); this is also evident from the apparently higher $E_{k\mathrm{Pg}}$ values than E_{kf} values ($P < 0.001$). Irrespective of tissue type, there was no significant correlation between gross photosynthesis rate and rETR. Figure 6a, b also emphasises this non-linearity between rETR and gross photosynthesis rate.

Sun- and shade-adapted regions of both coenosarc and polyp tissues showed a linear correlation between gross photosynthesis rate and O_2 concentration ($r^2 > 0.89$) with sun-adapted polyps showing a higher linear increase ($a = 0.069$) than shade-adapted polyps

Table 1 Differences in F_v/F_m, and Φ_{PSII} and non-photochemical quenching (NPQ) of sun- and shade-adapted coenosarc and polyp tissues of *Pocillopora damicornis* determined at 358 and 328 μmol photons m^{-2} s^{-1} for sun- and shade-adapted coenosarc tissues, respectively, and at 406 and 290 μmol photons m^{-2} s^{-1} for sun- and shade-adapted polyp tissues, respectively. Averages (n = 5 ± SE) are shown

	Coenosarc		Polyp		*P*-value
	Sun	Shade	Sun	Shade	
F_v/F_m	0.672 ± 0.016	0.695 ± 0.016	0.565 ± 0.038	0.576 ± 0.087	0.064
Φ_{PSII}	0.404^{a} ± 0.035	0.156^{b} ± 0.050	$0.172^{a,b,c}$ ± 0.048	0.095^{c} ± 0.061	**< 0.001**
NPQ	0.793 ± 0.225	6.210 ± 2.191	3.952 ± 1.876	5.717 ± 2.346	0.092

Tukey's post hoc comparisons ($P < 0.05$) between sun- and shade-adapted regions of coenosarc and polyp tissue are indicated with superscript letters. Significant *P*-value is bolded

Table 2 Quantitative parameters derived from fitted relative electron transport rates (rETR) and gross photosynthesis rate curves as a function of PAR

Parameter	Coenosarc		Polyp		*P*-value
	Sun	Shade	Sun	Shade	
$rETR_{max}$	136^{a} ± 14	77^{b} ± 13	$84^{a,b,c}$ ± 15	41^{c} ± 10	**< 0.001**
α_f	1.09^{a} ± 0.06	1.34^{b} ± 0.06	0.83^{c} ± 0.12	0.97^{a} ± 0.14	**0.023**
E_{kf}	$129^{a,b}$ ± 19	$58^{b,c}$ ± 31	$129^{a,b}$ ± 47	47^{c} ± 12	**0.016**
Pg_{max}	16 ± 5	21 ± 4	27 ± 6	12 ± 6	0.227
α_{Pg}	0.08 ± 0.02	0.16 ± 0.03	0.15 ± 0.05	0.12 ± 0.05	0.381
E_{kPg}	233 ± 56	158 ± 37	220 ± 73	104 ± 37	0.128

Variable chlorophyll α fluorescence—$rETR_{max}$ (a.u), α_f, E_{kf} (μmol photons m^{-2} s^{-1}); gross photosynthesis rate—Pg_{max} (nmol cm^{-3} s^{-1}), α_{Pg}, E_{kPg} (μmol photons m^{-2} s^{-1}). Values for sun- and shade-adapted coenosarc and polyp tissues are given. Averages (n = 5 ± SE) are shown. Tukey's post hoc comparisons ($P < 0.05$) between sun- and shade-adapted regions of coenosarc and polyp tissue are indicated with superscript letters. Significant *P*-value is bolded

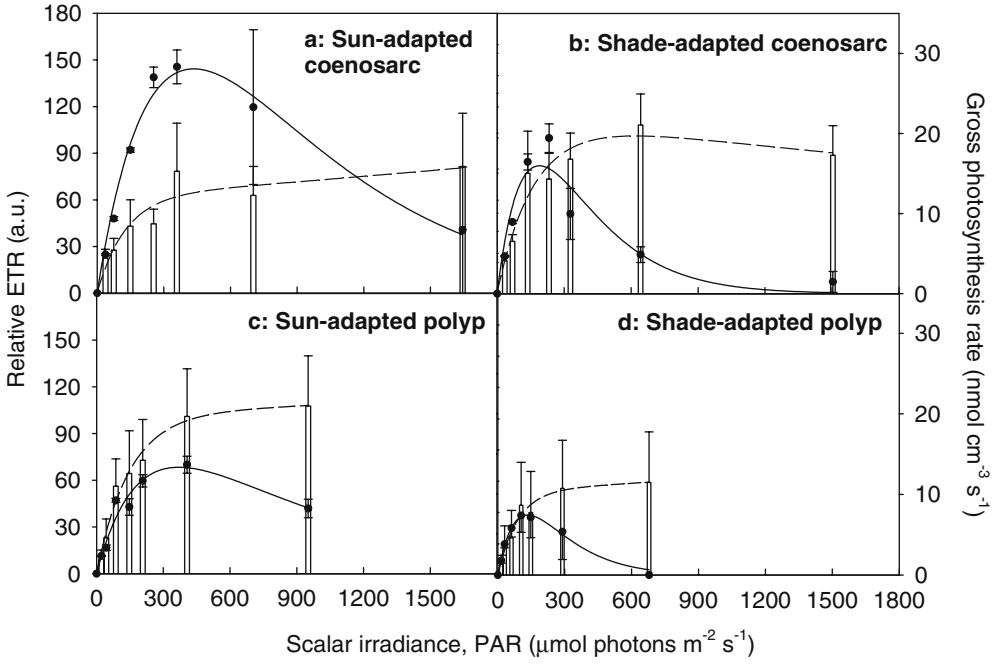

Fig. 5 Steady-state relative electron transport rate (rETR) (*filled circle*) and gross photosynthesis rate (*bars*) as a function of increasing scalar irradiance (μmol photons m^{-2} s^{-1}) of sun- (**a**) and shade-adapted (**b**) coenosarc and sun- (**c**) and shade-adapted (**d**) polyp tissues of *Pocillopora damicornis* (n = 5 ± SE). The fitted rETR curve is superimposed with a *solid line*. The fitted gross photosynthesis rate curve is superimposed with a *broken line*

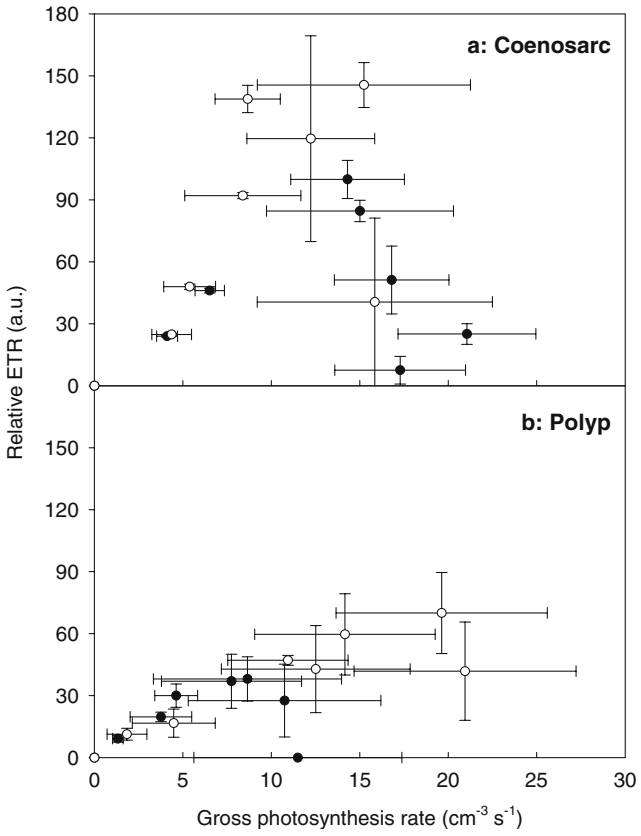

Fig. 6 Steady-state relative electron transport rate and gross photosynthesis rate of sun- (*empty circle*) and shade-adapted (*filled circle*) of coenosarc (**a**) and polyp (**b**) tissues of *Pocillopora damicornis* in response to increasing scalar irradiance ($n = 5 \pm$ SE)

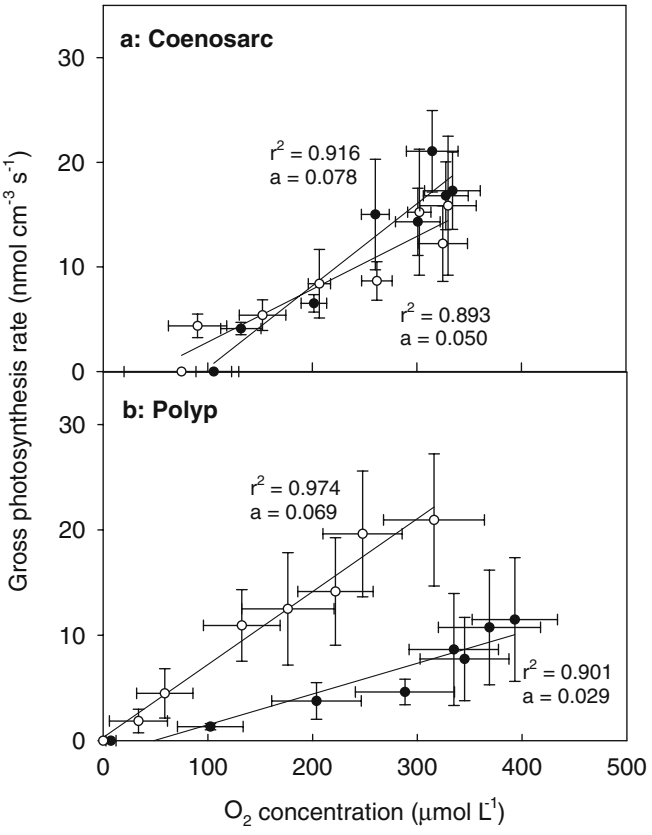

Fig. 7 Gross photosynthesis rate and O_2 concentration of sun- (*empty circle*) and shade-adapted (*filled circle*) coenosarc (**a**) and polyp (**b**) tissues of *Pocillopora damicornis* in response to increasing scalar irradiance ($n = 5 \pm$ SE). r^2, correlation coefficient; *a*, slope of the correlation line

($a = 0.029$) (Fig. 7b). Pearson's correlation coefficients between gross photosynthesis rates and O_2 concentrations were significant in sun- and shade-adapted tissue of coenosarc tissue ($P < 0.001$) as well as for sun- and shade-adapted polyps tissue ($P < 0.01$) (data not shown).

In coenosarc tissue, there was a linear relationship between rETR and O_2 concentration until ~300 µmol l^{-1} O_2, after which rETR decreased rapidly for both sun- and shade-adapted regions while the O_2 concentration ceased to increase (Fig. 8a). In polyp tissues, the decline of rETR occurred at ~250 µmol l^{-1} O_2 for sun-adapted regions and at 325 µmol l^{-1} O_2 for shade-adapted regions (Fig. 8b). Sun-adapted coenosarc and polyp tissues reached higher rETR values than shade-adapted tissues. In shade-adapted polyp tissues there was a trend towards higher O_2 levels than in sun-adapted tissue polyps.

Discussion

While microsensors for oxygen and variable chlorophyll *a* fluorescence have previously been employed separately to investigate the heterogeneity of zooxanthellae photosynthesis *in hospite* (Kühl et al. 1995; Ralph et al. 2002), this study provides the first combined microscale measurements of scalar irradiance, steady-state O_2 concentration, gross photosynthesis rates and PSII quantum yields and rETR in coral tissues. This is a major technical advance in coral photobiology. Variable fluorescence-based studies of corals are often used to infer impacts on the regulation of photosynthesis, yet hitherto no studies have actually compared steady-state photosynthesis rates with fluorescence-derived measures of coral photosynthesis obtained at similar spatial scales and within the same tissue type.

Light microclimate

Shallow-water corals such as those in the Heron Island lagoon are adapted to high irradiance, which may reach >2,000 µmol photons m^{-2} s^{-1} under light fleck conditions. However, zooxanthellae live in a diffuse light field where they receive a major part of the light for photosynthesis as scattered light through their calcium carbonate skeleton and within the tissue (Kühl et al. 1995; Enriquez et al. 2005). Multiple scattering in corals induces changes in the light field due to photon trapping (Kühl and Jørgensen 1994), which can increase the absorption efficiency of pigments significantly (Enriquez

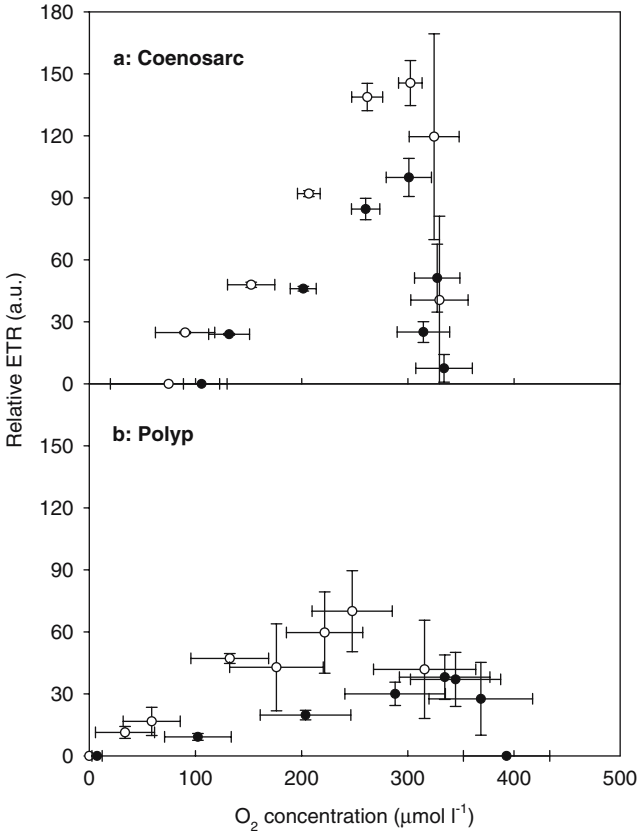

Fig. 8 Steady-state relative electron transport rate of sun- (*empty circle*) and shade-adapted (*filled circle*) of coenosarc (**a**) and polyp (**b**) tissues of *Pocillopora damicornis* as a function of O_2 concentration ($n = 5 \pm$ SE)

et al. 2005). The pigmentation of the coral tissue is critical to light-associated measurements such as variable chlorophyll *a* fluorescence measurements. Due to a strong contribution of multiple scattering by the skeleton (Enriquez et al. 2005), a highly pigmented area may induce less scattering of light than a more translucent tissue region. Similarly, fluorescence in lightly pigmented tissues may also be affected by multiple scattering. How these phenomena affect the measured fluorescence yields is yet to be determined.

The absorption maximum of chlorophyll *a* at 675 nm in the sun- and shade-adapted polyps was similar, but at other wavelengths the absorption varied significantly: overall absorption was higher in shade-adapted than in sun-adapted polyps and coenosarc tissue (Fig. 3). The percentage of incident downwelling light absorbed would be expected to correlate with the product of the zooxanthellae areal density and the cellular pigment content (Falkowski et al. 1984; Stambler and Dubinsky 2004) although multiple scattering by the skeleton enhancing the light field should also be taken into account (Enriquez et al. 2005).

Surface scalar irradiance measurements of coenosarc tissues ranged from 120 to 180% of the incident irradiance between 450 and 750 nm, with little spectral difference observed between sun- and shade-adapted coenosarc tissues or sun-adapted polyp tissues. However, the differences in scalar irradiance measured between coenosarc and polyp tissues as well as between sun- and shade-adapted polyp tissues (Fig. 3), highlight the importance and need for light measurements to accurately determine the light microclimate, which is likely to be significantly different from the light climate measured on the tissue surface.

Oxygen dynamics

The O_2 concentration at the coenosarc tissue surfaces (Fig. 4a) saturated at high irradiances, whereas polyp tissues did not fully saturate within the irradiance range of the experiment (Fig. 4b). This indicates that polyp tissues harbour zooxanthellae, which can retain photosynthetic activity at higher irradiance, e.g. in deeper parts of the polyp, where light is attenuated. In addition, oxygen produced in the thicker polyp tissues has a longer diffusion path and must cross a thicker DBL than oxygen produced in the coenosarc tissue and this may prolong the onset of O_2 saturation measured at the tissue surface (Kühl et al. 1996; Stambler and Dubinsky 2004). The retraction of polyp tissues at high irradiances (Brown et al. 2002) and the immobility of coenosarc tissues suggest that zooxanthellae harboured in coenosarc tissues are less shaded and must have greater capacity to cope with high irradiances than polyp tissues (Ralph et al. 2002). The maximum O_2 concentration obtained in sun-adapted polyp tissues was lower than in shade-adapted polyps (Fig. 4a) possibly due to a lower density of zooxanthellae in sun-adapted tissues (Falkowski et al. 1984) resulting in lower absorption of incident light (Fig. 3; Stambler and Dubinsky 2004).

We did not quantify respiration in our study. However, respiration in sun-adapted polyps is typically greater than in shade-adapted polyps (Coles and Jokiel 1977; Gattuso and Jaubert 1990) resulting in lower net oxygen production. While polyp tissues were severely O_2 depleted after 10 min of darkness, the coenosarc tissues retained a minimum O_2 level of $36 \pm 26\%$ saturation (Fig. 4a, b). Polyp tissues are highly mobile and may, therefore, exhibit higher respiration than coenosarc tissue. The differences in oxygen dynamics between coenosarc and polyp tissue are, however, also due to boundary layer effects. The interaction of flow and coral topography causes heterogeneous and complex DBLs over coral tissues (Kühl et al. 1995). Thicker boundary layers occurring over polyp tissues as compared to coenosarc tissues (Shashar et al. 1993) cause a more severe mass transfer limitation resulting in faster oxygen depletion and lower oxygen levels in the polyp tissue during darkness (Fig. 4). Corals can alleviate such mass transfer limitation by expanding their polyp tissues during night-time (Patterson 1992).

The higher compensation irradiance of sun-adapted than of shade-adapted tissues also indicates that more O_2 is consumed through respiration in high-light adap-

ted tissues (Fig. 4a, b) (Coles and Jokiel 1977; Gattuso and Jaubert 1990). Both coenosarc and polyp tissues, irrespective of orientation, were supersaturated with O_2 in moderate light (<190 µmol photons m^{-2} s^{-1}) and the steady-state O_2 curves (Fig. 4a, b) remained stable showing no indication of increasing oxygen consumption and/or decreasing photosynthesis (Fig. 5) at high scalar irradiance. Kühl et al. (1995) found no sign of photoinhibition in an *Acropora* species even at irradiances $>2{,}000$ µmol photons m^{-2} s^{-1}. This indicates that zooxanthellae can remain actively photosynthesising over a wide irradiance range, but see our caution about ETR measurements below. Whether this capacity is mainly physiological or is at least in part due to host factors such as protective pigments (Salih et al. 2000), alleviation of inhibitory irradiances due to tissue contraction and other issues related to the optical properties of the tissue, remains to be studied in further detail. The population of *P. damicornis* colonies at Heron Island harbours a genetically uniform but physiologically flexible zooxanthellar community with regard to photoacclimation. Such flexibility could be of vital significance following bleaching events where corals have lost symbionts due to combined changes to light and temperature conditions (Baker et al. 2004).

Steady-state relationships of gross photosynthesis rate, O_2 concentration and rETR

The linear correlation between gross photosynthesis rates and O_2 concentration (Fig. 7) coupled with the difference observed in O_2 concentration with increasing scalar irradiance in sun-adapted polyp tissues (Fig. 4b), confirms that oxygen consumption is relatively higher in sun-adapted compared to shade-adapted polyp tissues. This is also reflected in the slope of the correlation line of gross photosynthesis rate in sun-adapted polyps as a function of O_2 concentration, which was more than twice that of shade-adapted polyps (Fig. 7b).

In contrast to the high gross photosynthesis rates and O_2 concentration observed at high scalar irradiances, shade-adapted coenosarc and polyp tissues showed a decline in rETR over the course of the steady-state light curve, which would indicate that electron transport through the photosystems became severely restricted (Fig. 5b, d). The lack of correlation observed (Figs. 5, 6) suggests that variable chlorophyll *a* fluorescence measurements underestimated photosynthesis productivity in corals. Lack of correlation has previously been shown for free-living algae (Geel et al. 1997), a macroalga (Longstaff et al. 2003) as well as for higher plants (Harbinson et al. 1990) but in these cases rETR was higher than oxygen rates and several other studies have shown a good correlation between rETR and either ^{14}C- or O_2 production-based measurements of photosynthesis. Thus, the mismatch between rETR and gross photosynthetic O_2 production in corals is an important observation. Variable chlorophyll *a* fluorescence-derived measures of photosynthesis are often used as a proxy for photosynthetic competence and primary production, e.g. in connection with coral bleaching studies. In the following we discuss some possible mechanisms for the observed lack of correlation.

The non-linearity observed between combined measurements of O_2 and rETR are reflected as a dramatic decrease in rETR of the coral tissue at $[O_2]$ ~250–325 µmol l^{-1} (Fig. 8). This observation suggests that an alternate pathway for electron transport is entrained rather than being a product of greater respiration, photorespiration (Schnitzler-Parker et al. 2004) or photo-inactivation. It is unlikely that the Mehler ascorbate-peroxidase (MAP) reaction, which has oxygen as a terminal electron acceptor (Geel et al. 1997; Asada 1999) can account for this effect since the net oxygen production from water is offset completely by the uptake of oxygen in the MAP reaction and therefore oxygen exchange is zero. Here, there must be a flow of electrons to a sink that is maintaining a high rate of oxygen evolution which is apparently not measured by the PAM system at high irradiances. Down regulation of absorbed light energy through the xanthophyll cycle would be a sink for light energy but not for electrons. Thus the only other electron pathway that could possibly cause such an alteration to the relationship between O_2 synthesis and rETR appears to be cyclic PSII electron flow (Lavaud et al. 2002; Franklin and Badger 2001; Longstaff et al. 2002). Variable chlorophyll *a* fluorescence monitors only the rate of charge separation of PSII reaction centres leading to electron transport, which may not necessarily correlate directly to O_2 evolution. Also, there is no correlation between decreasing rETR at high irradiance (Fig. 5a–d) and increased non-photochemical quenching in coenosarc tissue (Table 1). This also suggests that there is non-cyclic ETR in PSII. Nevertheless, it is curious that oxygen evolution appears to be proceeding at near maximum rates while the electron transport rate approaches zero.

Our combined measurements were done with the tip of the oxygen microelectrode and the microfibre positioned at the tissue surface. Discrepancies between surface measurements of variable fluorescence and "true" photosynthesis rate have been investigated in some detail by researchers using such techniques to assess microphytobenthos productivity (Perkins et al. 2002; Forster and Kromkamp 2004) and our observations could in part be due to similar effects. The steady-state oxygen level measured at the tissue surface is an integral measure of net balance of photosynthesis and respiration in the tissue below. In contrast, the gross photosynthesis measurement has a spatial resolution of about 100 µm (Revsbech and Jørgensen 1983) and thus quantifies zooxanthellar photosynthesis close to the tissue surface. The microfibre probe measures chlorophyll *a* fluorescence in front of the fibre tip. The volume from which fluorescence is sampled depends on the optical properties of the tissue. In less pigmented more translucent tissues variable fluorescence from a larger tissue

volume is sampled as compared with measurements on the surface of tissues with a higher pigment density and/or with the zooxanthellae positioned further from the tissue surface. A decrease in relative ETR at higher irradiance could thus be due to contraction of tissue with zooxanthellae or full inhibition of zooxanthellae close to the tissue surface, while fluorescence from zooxanthellae in deeper layers is not detected by the microfibre. Such mechanisms would, however, be most pronounced in polyp tissue and cannot explain the decrease in rETR observed in the less contractile and more optically transparent coenosarc tissue. Furthermore, our O_2 microelectrode measurements showed no inhibition of gross photosynthesis close to the tissue surface. Clearly, there is a need for a closer investigation of this interesting phenomenon in corals.

Conclusion

The ability of coral polyps to contract and expand with environmental and physical stimuli has been shown to affect the local microenvironment (Kühl et al. 1995). The present study showed that, combined microsensor measurements were generally more variable in polyp tissues. The relationship between the estimated rate of relative PSII electron transport and the gross photosynthesis rate as well as O_2 concentration was found to be non-linear at high irradiances. Data obtained using variable fluorescence, especially in light stress conditions should thus be interpreted with caution and not be assumed to represent productivity. Further studies are needed to resolve the apparent discrepancy between photosynthetic oxygen production and fluorescence-derived measures of the rate of charge separation at PSII. Meanwhile, we caution against direct extrapolation of variable fluorescence data to actual rates of photosynthesis in corals exposed to high irradiance.

Acknowledgements We thank A. Glud for microsensor construction, N. Ralph for fabricating the flow-through chamber, and Dr B. Kelaher for advice on statistical data processing. We thank S.H. Magnusson for assistance with collecting the scalar irradiance data. We acknowledge R. Hill for editorial comments on drafts of the manuscript and the Department of Environmental Science, UTS and all staff at Heron Island Research Station for support. The research was funded jointly by a GBRMPA Science for Management award and a PADI grant to KEU, a UTS institutional grant to PJR, grants from the Australian Research Council to AWDL and PJR, and a grant from the Danish Natural Science Research Council to MK. The research was conducted under GBRMPA permit number G04/12776.1. This is contribution number 207 from the Institute of Water and Resource Management.

References

Asada K (1999) The water–water cycle in chloroplasts: scavenging of active oxygen and dissipation of excess photons. Annu Rev Plant Physiol Plant Mol Biol 50:601–639

Baker AC, Starger CJ, McClanahan TR, Glynn PW (2004) Corals' adaptive response to climate. Nature 430:741

Bhagooli R, Hidaka M (2003) Comparison of stress susceptibility of *in hospite* and isolated zooxanthellae among five coral species. J Exp Mar Biol Ecol 291:181–197

Brown BE, Downs CA, Dunne RP, Gibb SW (2002) Preliminary evidence for tissue retraction as a factor in photoprotection of corals incapable of xanthophyll cycling. J Exp Mar Biol Ecol 277:129–144

Buddemeier RW, Fautin DG (1993) Coral bleaching as an adaptive mechanism. BioScience 48:320–326

Coles SL, Jokiel PL (1977) Effects of temperature on photosynthesis and respiration in hermatypic corals. Mar Biol 43:209–216

De Beer D, Kühl M, Stambler N, Vaki L (2000) A microsensor study of light enhanced Ca^{2+} uptake and photosynthesis in the reef-building coral *Favia* sp. Mar Ecol Prog Ser 194:75–85

Dubinsky Z, Falkowski PG, Porter JW, Muscatine L (1984) Absorption and utilization of radiant energy by light- and shade adapted colonies of the hermatypic coral *Stylophora pistillata*. Proc R Soc Lond B 222:203–214

Enriquez S, Méndez ER, Iglesias-Prieto R (2005) Multiple scattering on coral skeletons enhances light absorption by symbiotic algae. Limnol Oceanogr 50(4):1025–1032

Falkowski PG, Dubinsky Z, Muscatine L, Porter JW (1984) Light and the bioenergetics of a symbiotic coral. BioScience 34:705–709

Falkowski PG, Jokiel PL, Kinzie RA (1990) Irradiance and corals. In: Dubinsky Z (ed) Ecosystems of the World 25: Coral Reefs. Elsevier, Amsterdam, pp 89–107

Forster RM, Kromkamp JC (2004) Modelling the effects of chlorophyll fluorescence from subsurface layers on photosynthetic efficiency measurements in microphytobenthic algae. Mar Ecol Prog Ser 284:9–22

Franklin LA, Badger MR (2001) A comparison of photosynthetic electron transport rates in macroalgae measured by pulse amplitude modulated chlorophyll fluorometry and mass spectrometry. J Phycol 37:756–767

Gattuso J-P, Jaubert J (1990) Effect of light on oxygen and carbon dioxide fluxes and on metabolic quotients measured *in situ* in a zooxanthellate coral. Limnol Oceanogr 35(8):1796–1804

Geel C, Versluis W, Snel JFH (1997) Estimation of oxygen evolution by marine phytoplankton from measurements of the efficiency of photosystem II electron flow. Photosynth Res 51:61–70

Harbinson J, Genty B, Baker NR (1990) The relationship between CO_2 assimilation and electron transport in leaves. Photosynth Res 25:213–224

Hill R, Schreiber U, Gademann R, Larkum AWD, Kühl M, Ralph PJ (2004) Spatial heterogeneity of photosynthesis and the effect of temperature-induced bleaching conditions in three species of coral. Mar Biol 144:633–640

Hoegh-Guldberg O (1999) Climate change, coral bleaching and the future of the world's coral reefs. Mar Freshw Res 50:839–869

Jones RJ, Hoegh-Guldberg O, Larkum AWD, Schreiber U (1998) Temperature-induced bleaching of corals begins with impairment of the CO_2 mechanism in zooxanthellae. Plant Cell Environ 21:1219–1230

Kühl M (2005) Optical microsensors for analysis of microbial communities. Methods Enzymol 397:166–199

Kühl M, Jørgensen BB (1994) The light field of micro-benthic communities: radiance distribution and microscale optics of sandy coastal sediments. Limnol Oceanogr 39:1368–1398

Kühl M, Cohen Y, Dalsgaard T, Jørgensen BB, Revsbech NP (1995) Microenvironment and photosynthesis of zooxanthellae in scleractinian corals studies with microsensors for O_2, pH and light. Mar Ecol Prog Ser 117:159–172

Kühl M, Glud RN, Ploug H, Ramsing NB (1996) Microenvironmental control of photosynthesis and photosynthesis-coupled respiration in an epilithic cyanobacterial biofilm. J Phycol 32:799–812

Kühl M, Glud RN, Borum J, Roberts R, Rysgaard S (2001) Photosynthetic performance of surface associated algae below sea ice as measured with a pulse amplitude modulated (PAM) fluorometer and O_2 microsensors. Mar Ecol Prog Ser 223:1–14

LaJeunesse TC, Loh WKW, van Woesik R (2003) Low symbiont diversity in southern Great Barrier Reef corals, relative to those of the Caribbean. Limnol Oceanogr 48(5):2046–2054

Lassen C, Plough H, Jørgensen BB (1992) A fibre-optic scalar irradiance microsensor: application for spectral light measurements in sediments. FEMS Microbiol Ecol 86:247–254

Lavaud J, van Gorkom H, Etienne A (2002) Photosystem II electron transfer cycle and chlororespiration in planktonic diatoms. Photosynth Res 74:51–59

Lesser MP, Mazel C, Phinney D, Yentsch CS (2000) Light absorption and utilization by colonies of the congeneric hermatypic corals *Montastraea faveolata* and *Montastraea cavernosa*. Limnol Oceanogr 45(1):76–86

Longstaff BJ, Kildea T, Runcie JW, Cheshire A, Dennison WC, Hurd C, Kana T, Raven JA, Larkum AWD (2002) An *in situ* study of photosynthetic oxygen exchange and electron transport rate in the marine macroalga *Ulva lactuca* (Chlorophyta). Photosynth Res 74:281–293

Lorenzen J, Glud R, Revsbech NP (1995) Impact of microsensor-caused changes in diffusive boundary layer thickness on O_2 profiles and photosynthetic rates in benthic communities of microorganisms. Mar Ecol Prog Ser 199:237–241

Marshall PA, Baird AH (2000) Bleaching of corals on the Great Barrier Reef: differential susceptibilities among taxa. Coral Reefs 19:155–163

Patterson MR (1992) A chemical engineering view of cnidarian symbioses. Am Zool 32(4):566–582

Patterson MR, Sebens KP, Olson RR (1991) *In situ* measurements of flow effects on primary production and dark respiration in reef corals. Limnol Oceanogr 36:936–948

Perkins RG, Oxborough K, Hanlon ARM, Underwood GJC, Baker NR (2002) Can chlorophyll fluorescence be used to estimate the rate of photosynthetic electron transport within microphytobenthic biofilms. Mar Ecol Prog Ser 228:47–56

Platt T, Gallegos CL, Harrison WG (1980) Photoinhibition of photosynthesis in natural assemblages of marine phytoplankton. J Mar Res 38:687–701

Ralph PJ, Gademann R (2005) Rapid light curves: a powerful tool for the assessment of photosynthetic activity. Aquat Bot 82:222–237

Ralph PJ, Gademann R, Larkum AWD, Kühl M (2002) Spatial heterogeneity in active chlorophyll fluorescence and PSII activity of coral tissues. Mar Biol 141:639–646

Ralph PJ, Schreiber U, Gademann R, Kühl M, Larkum AWD (2005) Coral photobiology studied with a new imaging pulse amplitude modulated fluorometer. J Phycol 41:335–342

Revsbech NP (1989) An oxygen microelectrode with a guard cathode. Limnol Oceanogr 34:474–478

Revsbech NP, Jørgensen BB (1983) Photosynthesis of benthic microflora measured with high spatial resolution by the oxygen microprofile method: capabilities and limitations of the method. Limnol Oceanogr 28:749–756

Salih A, Larkum AWD, Cox G, Kühl M, Hoegh-Guldberg O (2000) Fluorescent pigments in corals are photoprotective. Nature 408:850–853

Schnitzler-Parker M, Armbrust EV, Piovia-Scott J, Keil RG (2004) Induction of photorespiration by light in the centric diatom *Thalassiosira weissflogii* (Bacillariopyceae): molecular characterization and physiological consequences. J Phycol 40:557–567

Schreiber U (2004) Pulse-amplitude-modulation (PAM) fluorometry and saturation pulse method: an overview. In: Papageorgiou GC, Govindjee (eds) Chlorophyll fluorescence: a signature of photosynthesis. Kluwer Academic Publishers, Dordrecht, pp. 279–319

Schreiber U, Kühl M, Klimant I, Reising H (1996) Measurement of chlorophyll fluorescence within leaves using a modified PAM fluorometer with a fiber-optic microprobe. Photosynth Res 47:103–109

Shashar N, Cohen Y, Loya Y (1993) Extreme fluctuations of oxygen in diffusive boundary layers surrounding stony corals. Biol Bull 185:455–461

Stambler N, Dubinsky Z (2004) Corals as light collectors: an integrating sphere approach. Coral Reefs 24(1):1–9

Ulstrup KE, Hill R, Ralph PJ (2005) Photosynthetic impact of hypoxia on *in hospite* zooxanthellae in the scleractinian coral *Pocillopora damicornis*. Mar Ecol Prog Ser 286:125–132

Ulstrup KE, Berkelmans R, Ralph PJ, van Oppen MJH (2006) Variation in bleaching sensitivity of two coral species with contrasting bleaching thresholds across a latitudinal gradient on the GBR. Mar Ecol Prog Ser (in press)

Warner ME, Fitt WK, Schmidt GW (1999) Damage to photosystem II in symbiotic dinoflagellates: a determinant bleaching. Proc Natl Acad Sci USA 96:8007–8012